

SolarPACES 2013

Advanced CFD&HT numerical modeling of solar tower receivers

G. Colomer^a, J. Chiva^b, O. Lehmkuhl^{a,b} and A. Oliva^b

^aTermo Fluids S.L., Avinguda Jaquard, 97 1-E, 08222, Terrassa, Barcelona, Spain, E-mail: termofluids@termofluids.com

^bHeat and Mass Transfer Technological Center (CTTC), Universitat Politècnica de Catalunya-BarcelonaTech (UPC), ETSEIAT Colom 11, 08222, Terrassa, Spain. Phone: +34 937398192, Fax: +34 93 7398020, E-mail: cttc@cttc.upc.edu

Abstract

This paper presents an advanced methodology for the detailed modeling of the heat transfer and fluid dynamics phenomena in solar tower receivers. It has been carried out in the framework of a more ambitious enterprise which aims at modeling all the complex heat transfer and fluid dynamics phenomena present in central solar receivers. The global model is composed of 4 sub-models (heat conduction, two-phase flow, thermal radiation and natural convection) which are described. Results of the numerical model obtained so far are also presented and discussed

© 2013 The Authors. Published by Elsevier Ltd. This is an open access article under the CC BY-NC-ND license (<http://creativecommons.org/licenses/by-nc-nd/3.0/>).

Selection and peer review by the scientific conference committee of SolarPACES 2013 under responsibility of PSE AG.

Final manuscript published as received without editorial corrections.

Keywords: numerical model; solar tower; CFD&HT

1. Introduction

Solar thermal energy is becoming a very important renewable energy, with large scale plants operating in different parts of the world [1]. There are different designs for solar power collectors that are currently being used to generate electricity, like parabolic trough, parabolic dish and solar tower. In a solar tower plant, the solar radiation is reflected and concentrated by a field of mirrors into a receiver. Panels of tubes with circulating water receive this radiation and steam is produced. This steam is used to power turbines in order to generate electrical energy. The heat transfer and fluid dynamics phenomena in the receiver are the interest of this study. The purpose of the current work is to describe the numerical model of a saturated steam solar receiver, which includes sub-models for heat conduction, two-phase flow, solar and thermal radiation and turbulent natural convection.

TermoFluids [2], a general purpose unstructured and parallel object-oriented CFD code developed to solve industrial flows, is used in this work.

2. Definition of the modeling

A scheme of a solar tower field is given in Fig. 1a. The receiver is composed essentially by an array of tubes but different designs for the tubes and the structure of the receiver are considered in the model (tubes with fins, different angles, grouped in panels, inside a cavity, cylindrical, with or without back-insulation, more than one level of arrays, etc.). Two possible configurations are shown in Fig. 1b (horizontal finned tubes inside a cavity with back-insulation) and Fig. 1c (portion of a cylindrical receiver with vertical tubes and back-insulation).

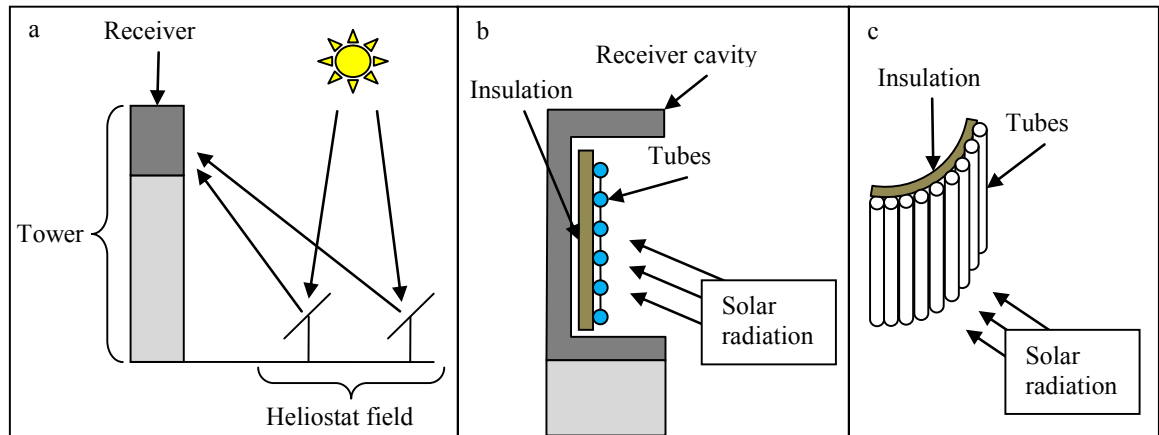


Fig. 1. (a) Scheme of a solar tower power plant. (b) Scheme of receiver cavity. (c) Scheme of a portion of a cylindrical receiver.

The mathematical model considers:

- Transient conduction heat transfer at the solid elements of the receiver (tubes shown in Fig. 1b and Fig. 1c).
- Two-phase flow inside the tubes of the receiver.
- Solar radiation received by the tubes.
- Radiative heat transfer between the surfaces of the receiver.
- Convective heat transfer between the tubes and the air surrounding them.

2.1. Heat conduction in the solid elements of the solar receiver

Transient conduction heat transfer can be solved directly from the governing equation. For the case of transient heat conduction without volumetric sources, the energy transport equation can be written in integral form as:

$$\rho c_p \frac{\partial T}{\partial t} = \nabla \cdot (\lambda \nabla T) \quad (1)$$

where T represents temperature, t is the time, ρ is density, c_p is the specific heat and λ the thermal conductivity. Unfortunately, due to the geometry of the receivers considered by the model presented, a correct evaluation of conduction heat transfer is not straightforward. The width of the tubes is of the order of millimetres while the overall receiver is of the order of meters. In order to solve eq. 1 using finite volume techniques, large meshes have to be used to solve the heat transfer at the tubes, and parallel computers are needed. In this work, a non-structured mesh has been used, so that extensions to other geometries of the tubes can be implemented without substantial changes. A parametric mesh generator has been designed and implemented in order to reduce the time needed to change the density of the mesh or the number of tubes. This program allows to obtain meshes with different densities and number of tubes and also to concentrate the control volumes at the critical points (for example, the union between tubes and fins of a receiver with that configuration).

In TernoFluids, for the integration of the governing equations the finite control volume method has been used. A modified least-square method has been chosen for the calculation of the gradients. The resulting system of equations is solved by means of the Conjugate Gradient method [2].

The conduction model links all the other models through boundary conditions:

- Insulation at the back side of the tubes: The back side of the tubes of the receiver may be covered with an insulating material. This situation is simulated using a one dimensional approach to obtain the value of the heat flux between the tubes and the air in contact with the insulating material:

$$q = \alpha \lambda \left(\frac{T_w - T_g}{\lambda + \alpha \Delta x} \right) \quad (2)$$

where q is the heat flux, α is the convective heat transfer coefficient, λ is the thermal conductivity of the insulator material, T_w and T_g are the temperature of the external wall of the tube and the temperature of the air respectively and Δx is the thickness of the insulator.

- Solar radiation at the tubes of the receiver: The radiation reflected by the heliostats to the receiver is distributed on the tubes. This distribution depends on the particular arrangement and the absorptivity of the tubes, and the incidence direction of the solar radiation. This input can be given to the convection-conduction simulation code.
- Thermal radiation at the surfaces of the receiver: the radiative heat transfer between the surfaces of the receiver can be calculated using the radiosity method, or using a Monte Carlo Ray Tracing (MCRT) tool. Using the former, more efficient method, the view factors are calculated by taking multiple reflections into account, and including the fact that any given tube will see only a part of some other tubes. A calculation using only the MCRT tool is possible, although significantly more expensive in terms of computational cost.
- The convective heat transfer between the tubes and the air of the cavity is calculated using the Newton's law of cooling:

$$q = \alpha(T_w - T_g) \quad (3)$$

and the convective heat transfer coefficient α is calculated from the Nusselt number (obtained as described in section 2.4):

$$\alpha = \frac{\lambda Nu}{L} \quad (4)$$

where λ is the thermal conductivity of the air and L is the characteristic length.

- Forced convection inside the tubes: The convective heat transfer between the internal flow of the fluid and the tubes of the panels is calculated using Newton's law of cooling. The temperature of the fluid and the convective heat transfer coefficient are obtained from the two-phase flow model described in next section.

2.2. Two-phase flow inside the tubes

The evaporation phenomena inside the tubes cannot be solved directly from the governing equations (mass, energy and momentum conservation), because instantaneous tracking of the vapor-liquid inter-phase is too complex to do so.

In this work, a one dimensional quasi-homogeneous model has been chosen to represent the forced convection in the tubes, solved by the step by step method, which was used in the numerical analysis of two-phase flow inside tubes [3]. The fact that this code is one dimensional makes difficult the communication between the two-phase flow code and the code for the solid elements. This problem has been solved calculating one heat transfer coefficient and one average wall temperature obtained from evaluating the energy conservation equation at the walls of the pipes.

For this model, the crux of the matter is the critical heat flux (CHF), an abrupt rise of wall temperature due to a slight change in one of the flow variables. The temperature rise may be of two or three orders of magnitude, which most likely will cause a failure of the heated surface. Finding the CHF in terms of saturated evaporation is not straightforward. There is a wide variety of correlations that try to predict this condition and the corresponding location of the point of dry-out inside pipes, but there is not a correlation that provides satisfactory results under different geometries and working conditions of the fluid. So far, the Look-up tables (LUT) method seems to be one that can give similar results to the experiments. Moreover, this method allows the extension of this application to different situations in a manner not too complicated. The implementation of this method in the code was made using the LUT of 2006 [4]. These tables are a function of pressure, mass flow and quality of steam. It is necessary to make a process of linear interpolation between the various tables that exist to find the CHF corresponding to the working conditions of the fluid.

The two-phase flow code has been validated with:

- Experimental data for low energy flow [5, 6, 7].
- Experimental data obtained at the CTTC laboratory using a vapor compression refrigeration system [8].
- Experimental data for high energy flow and correlations to predict the status of CHF [4, 9].

2.3. Radiation heat transfer modeling

The modeling of radiation heat transfer is carried out by means of an in-house MCRT tool [10] that follows the path of each sample photon accurately. This kind of tool is computationally expensive, because a high number of samples must be shot to reduce statistical errors. However, as each sample is independent of the others, this procedure can be efficiently parallelized either using multiple CPUs or dedicated GPUs. Because each sample is accurately ray-traced, multiple reflections of solar and thermal radiation that occur on the tubes and plates of the receivers of solar power plants are accounted for naturally. Thus, complex geometries of the receivers can be considered with a reasonable additional computational effort.

2.3.1. Solar radiation

The incident solar radiation is the required input condition for the simulation of the thermal behavior of the receiver of solar tower power plants. The distribution of the incoming intensity over the tubes of the receiver is estimated with the help of the MCRT tool and experimental knowledge. Several arrangements of the tubes, as well as incidence angles and tube properties can be easily tested.

With a ray tracing tool it is also possible, in theory, to obtain a more accurate distribution of the incident solar radiation on the receiver by taking into account the position of the sun and the distribution of the heliostats around the tower. However, due to the large number of heliostats, and to the large ratio between the sizes of the domain and the receiver, the computational cost would be too high. A future GPU implementation of the MCRT would perhaps make this simulation affordable. Therefore, in this work the amount of incident solar radiation per unit surface is taken from experimental knowledge alone.

2.3.2. Heat losses

The MCRT tool can also be used to calculate heat losses on the tubes due to emission of thermal radiation. For solar receivers designed to operate at high temperature, these losses can be significant.

In the MCRT approach, radiation heat balance on the receiver is computed in a simple way: on a first stage, the surface of every object used in the modelization of the receiver (a tube or a flat panel) is divided into a number of areas. Next, a number of samples are shot from all surfaces and from the sources that emulate the incident radiation coming from the mirrors. Experimental knowledge of the incoming intensity is required in this stage. All samples have equal energy. Then, the heat balance on a given area is the difference between the number of samples that are absorbed and emitted at that particular area, multiplied by the energy of the sample.

It should be noted that if an object is divided into a large number of areas, the heat flux distribution on its surface will be very detailed. On the other hand, a large number of areas results on higher fluctuations on the number of

samples that are absorbed at a particular area, thus requiring a larger number of samples to be shot in order to obtain meaningful heat flux values.

Heat losses due to emission of thermal radiation can also be taken into account by the radiosity method. In a general situation, this method requires the knowledge of the specular view factors [10] between all the objects considered in the simulation. The radiosity method is very fast when compared to the MCRT method, although the complication lies in the determination of the specular view factors. Fortunately, the specular view factors can be computed with MCRT techniques. The calculation is expensive in computational terms, but the accuracy can be traded by speed, as done for example by Miyanaga and Nakano [11]. The validity of this approach has been assessed in cases with radiation heat transfer coupled to laminar natural convection on a differential heated cavity (these results are not included in this work).

2.4. The convection outside the tubes

The temperature differences between the tubes and the air surrounding them produce heat transfer by convection. This heat transfer is complicated to evaluate numerically (the geometry is complex and there are large differences between the diameter of the tubes and their length, the air conditions in the real case are variable in time and space, the temperature differences between the tubes and the air are high, etc.).

TermoFluids considers the resolution of the three-dimensional Navier-Stokes equations by means of Large Eddy Simulation (LES) or Direct Numerical Simulation (DNS). Different models can be used for modeling subgrid-scale (SGS) tensor, e.g. the Wall-adapting eddy viscosity model (WALE [12]).

The governing equations used in TermoFluids have been discretized on a collocated unstructured grid arrangement by means of second-order spectra-consistent schemes. Such schemes are conservative, i.e. they preserve the kinetic energy equation. These conservation properties are held if, and only if the discrete convective operator is skew-symmetric, the negative conjugate transpose of the discrete gradient operator is exactly equal to the divergence operator and the diffusive operator, is symmetric and positive-definite. These properties ensure both, stability and conservation of the kinetic-energy balance even at high Reynolds numbers and with coarse grids [13]. For the temporal discretization, in TermoFluids different numerical schemes are considered, e.g. Runge-Kutta scheme [14].

From the CFD&HT numerical study local and average Nusselt number are obtained. These parameters are then used for evaluating the heat transfer coefficients required by the heat conduction model.

3. Illustrative results

3.1. Heat Conduction

In Fig. 2, an example of the distribution of dimensionless temperature is shown. This configuration corresponds with an array of tubes of a solar receiver with a similar design to the one depicted in Fig. 1b. Due to the incoming solar radiation, the temperature at the front side of the tubes is higher than that at the back side. As the fins between the tubes are not in direct contact with the circulating fluid inside the tubes they achieve high temperatures.

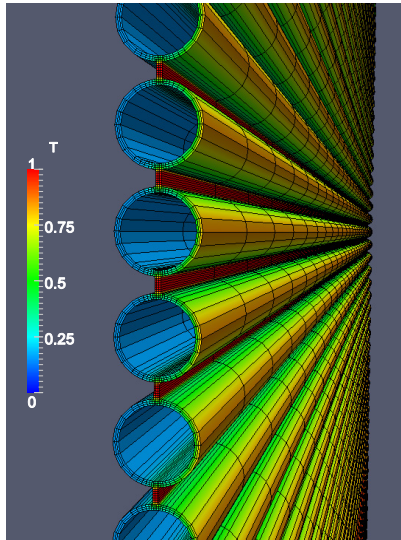


Fig. 2 Dimensionless distribution of temperature on a receiver formed by tubes with fins between them.

3.2. Radiation

An example of the calculation of an input condition that can be used on a convection-conduction simulation, Fig. 3a shows the distribution of incoming solar heat flux for a simplified circular receiver of a solar tower power plant. The absorptivity of the tubes is set to 0.9. A total of 0.32 billion samples were shot using 32 CPUs. The units are arbitrary, with red areas indicating the highest values of solar heat flux and blue areas indicating the zones with the lowest solar heat flux. As stated before, the effect of the heliostats on the incidence is not calculated, but assumed to provide a uniformly distributed intensity along the circumference of the receiver, and directed towards the vertical axis of the receiver, indicated by the red arrows in Fig. 3b. An inner cylindrical wall, not shown in the figure, reflects the incoming solar radiation back to the tubes. Note that there is some incident radiation on the side of the tubes facing the inner cylindrical wall.

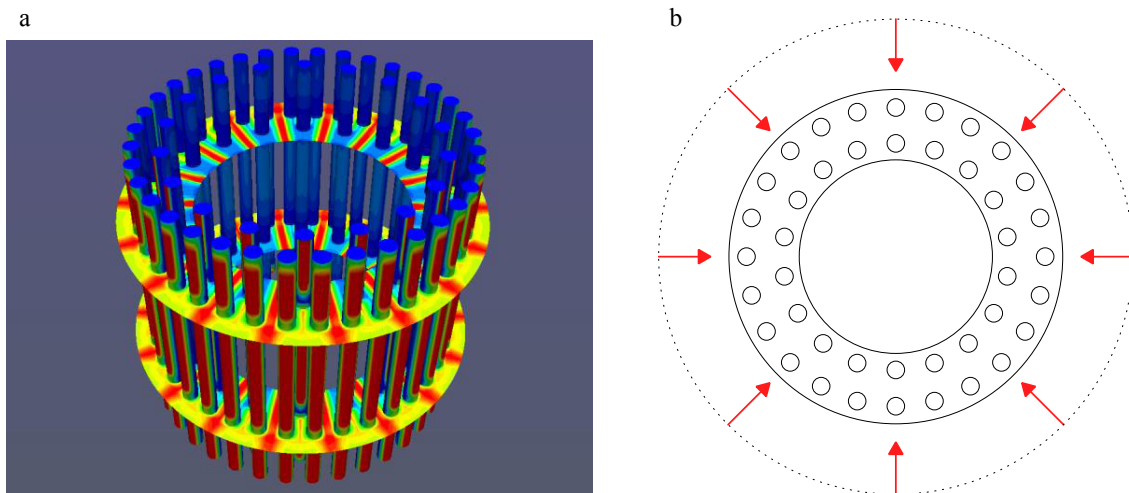


Fig. 3 (a) Distribution of solar heat flux on the tubes. (b) Top view of the receiver, indicating the direction of solar heat flux incidence resulting from the solar radiation being reflected by the heliostats.

3.3. Convection

In order to reduce the complexity of the problem some assumptions have been made:

- The panels of tubes have been modelled as a hot isothermal wall.
- Only natural convection occurs (no wind) and the temperature of the air away from the tubes is constant.
- The air has been supposed an incompressible Newtonian fluid, with constant thermophysical properties and negligible interaction in radiation.

Under these assumptions, direct numerical simulations of natural convection inside a simplified cavity of a solar tower receiver have been carried out to test the validity of the Boussinesq approximation when the temperature differences are high.

3.3.1. Problem definition an numerical domain

The situation under consideration in the simulations have been natural convection of air ($Pr = \nu/\alpha = 0.71$) in an *open cavity* (see Fig. 4a) with a Rayleigh number, based on the height of the cavity $H2$, of $Ra = g\beta(T_h - T_c)((H2)^3 Pr)/\nu^2 = 10^{12}$, a non-dimensional temperature difference value of $\varepsilon = (T_h - T_c)/(T_h + T_c) = 0.4$ and height aspect ratio $H2/L1 = 4$.

The vertical hot wall (identified with 2 in Fig. 4a) is considered isothermal with temperature $T_h = 686.35$ K. The top and bottom walls and the surfaces attached to them (corresponding with boundary 1 in Fig. 4a) are considered adiabatic. No slip conditions are set at the solid walls. The flow has been considered periodic in the z axis. Pressure boundary conditions are imposed at the top, bottom and left boundaries of the domain (boundary 3 in Fig. 4a), with Neumann condition for temperature if the air goes out of the system and temperature $T_c = 294.15$ K if it goes in.

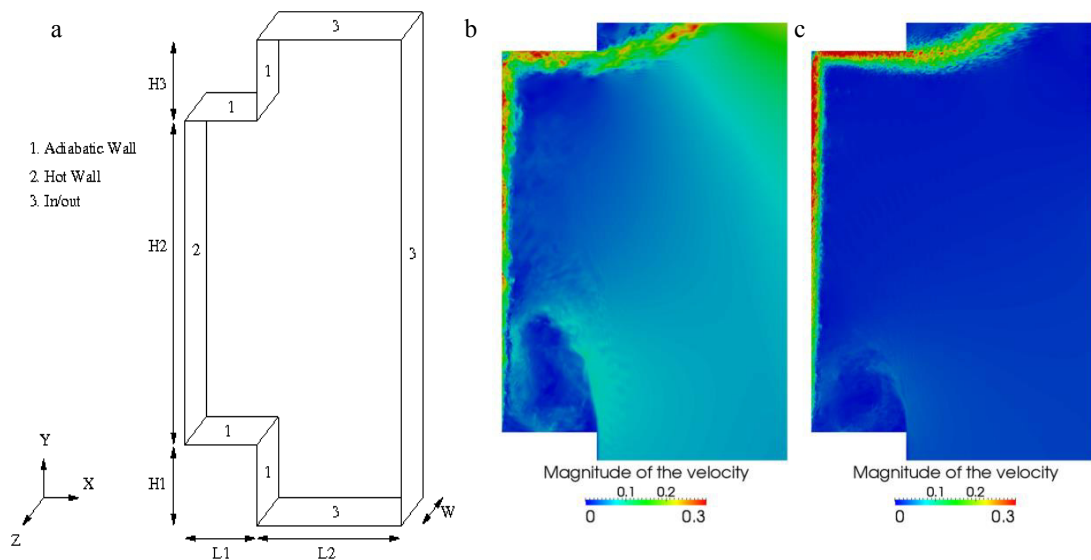


Fig. 4. (a) Scheme of the simplified solar receiver open cavity. 2D view at the symmetry plane of the instantaneous magnitude of the velocity: (b) Boussinesq approximation and (c) variable properties.

The meshes used for solving the domain considered have been generated by a constant step extrusion of a two-dimensional (2D) structured grid. Under these conditions, the span-wise coupling of the discrete Poisson equation, which results from the incompressibility constrain, yields circulant sub-matrices that are diagonalizable in a Fourier space. This allows to solve the Poisson equation by means of a Fast Fourier Transform (FFT) method. The algorithm used is based on the explicit calculation and direct solution of a Schur Complement system for the independent 2D systems. For more details the reader is referred to [15].

The number of control volumes of the final mesh has been 145,506 by 64 planes (about 9.3 million control volumes). In order to properly evaluate the boundary layer near the hot wall, a stretching has been applied to concentrate the maximum number of control volumes inside the boundary layer. The mesh size has been designed using knowledge from previous works [14, 16].

3.3.2. Results

In the present work, the results of direct numerical simulations considering constant (Boussinesq approximation) and variable thermo-physical properties have been compared. The simulations has been started with the air temperature set to T_c . Then, the simulation has been advanced in time until statistical stationary flow conditions have been achieved. After the initial transient has been completely washed out, averaged statistics have been computed.

3.3.2.1. Instantaneous flow

A comparison of the instantaneous magnitude of the velocity at the symmetry plane (Fig. 4b,c) shows clear differences between the two approaches. The values close to the hot wall and at the top of the cavity are higher with variable properties than with the Boussinesq approximation. Yet, in both cases, a small recirculation can be observed at the top corner of the cavity, caused by the ascension of thermal plumes next to the hot wall. There is also an entrainment of cold fluid from the bottom of the cavity which produces a recirculation which seems to be close to a quarter of the total height of the cavity ($H/2$). The interaction between the recirculation in this zone with the hot wall produces fluid instabilities at the bottom of the boundary layer, promoting the generation of turbulence.

3.3.2.2. Time-averaged statistics

Time-averaged statistics presented in this paper have been obtained by averaging the computed variables in time and homogeneous direction.

The recirculation between the hot wall and the bottom of the cavity observed from the analysis of the instantaneous flow is clearly represented by the stream lines in Fig. 5a,b. The center is situated at $x/L1 = 0.465$ and $y/L1 = 0.353$ with Boussinesq approximation and $x/L1 = 0.502$ and $y/L1 = 0.334$ with variable properties. Temperature contours are depicted in Fig. 5c,d. Temperature gradients can be seen over the whole cavity with Boussinesq approximation while it is not the case for variable properties.

The distributions of temperature variance in Fig. 6a,b show that there is some influence of the recirculation at the bottom with Boussinesq approximation, while with variable properties it is mainly concentrated close to the hot wall and at the top. The turbulent kinetic energy distributions depicted in Fig. 6c,d show higher values close to the hot wall and at the top of the cavity with variable properties and clear differences in the central region of the cavity between both approaches.

In Fig. 7 profiles of the averaged Nusselt number along the hot wall are shown. There is no transition point between laminar and turbulent regime as the flow is fully turbulent from the beginning due to the influence of the fluid entrainment from the bottom of the cavity. Near the top the Nusselt number manifests the behavior of impinging phenomena, where the temperature of the air gets closer to the temperature of the wall due to the collision of the vertical flow against the top of the cavity. The overall averaged Nusselt number is 978 with Boussinesq approximation and 1110 with variable properties. The conclusion obtained from the comparison of the averaged Nusselt number at the hot wall is that the convective heat transfer is underestimated when the Boussinesq approximation is used at high temperature differences.

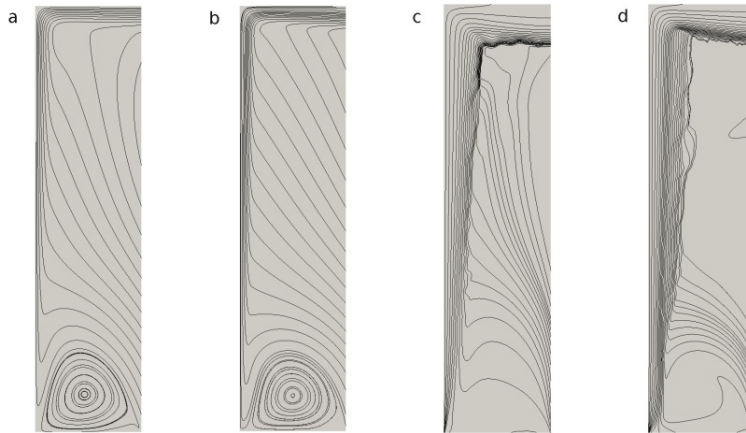


Fig. 5. Stream lines: (a) Boussinesq approximation, (b) variable properties. Temperature distribution: (c) Boussinesq approximation, (d) variable properties.

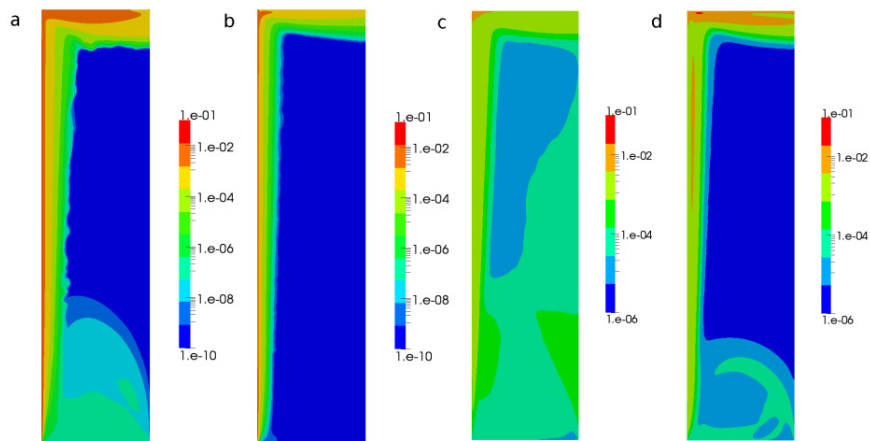


Fig. 6. Temperature variance: (a) Boussinesq approximation, (b) variable properties. Turbulent kinetic energy: (c) Boussinesq approximation, (d) variable properties.

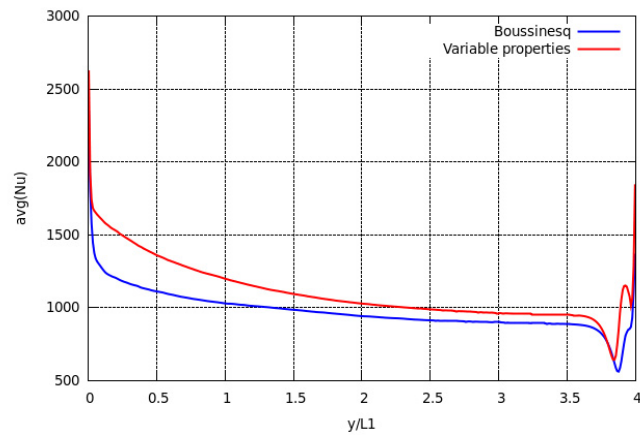


Fig. 7. Profiles of the averaged Nusselt number along the hot wall.

4. Towards the CFD&HT of full-scale solar tower receivers

The methodology to simulate heat transfer and fluid dynamics phenomena in the receiver of a solar tower has been presented. Models for the heat conduction in solids, two-phase flow, solar and thermal radiation and natural convection have been described and thoroughly validated against different experimental and numerical results.

The methodology presented above is currently being used for the CFD&HT modeling of a full-scale solar tower receiver. At the time this contribution is written, only a few instants of the complex unsteady fluid-dynamic and heat transfer phenomena have been simulated. More results will be presented at the congress.

Acknowledgements

This work has been financially supported by the Ministerio de Educación y Ciencia, Secretaría de Estado de Universidades e Investigación, Spain (ref. ENE2010-17801) and by the Collaboration Project between Universidad Politécnica de Catalunya and Termo Fluids S.L.

References

- [1] NREL, National Renewable Energy Laboratory. Concentrating Solar Power Projects, <http://www.nrel.gov/csp/solarpaces/>
- [2] Lehmkuhl O., Pérez Segarra C. D., Borrell R., Soria M. and Oliva A., 2007. TermoFluids: A new Parallel unstructured CFD code for the simulation of turbulent industrial problems on low cost PC Cluster. Proceedings of the Parallel CFD 2007 Conference, pg. 1-8.
- [3] Morales Ruiz S., Rigola J., Pérez Segarra C.D. and García Valladares O., 2008. Numerical analysis of two-phase flow in condensers and evaporators with special emphasis on single phase-two phase transition zones. Applied Thermal Engineering 29, pg. 1032-1042.
- [4] Groeneveld D.C., Shan J.Q., Vasic A.Z., Leung L.K.H., Durmayaz A., Yang J., Cheng S.C. and Tanase A., 2007. The 2006 CHF Look-up table, Nuclear Engineering and Design, vol 237, pg. 1909-1922.
- [5] Kattan N., Thome J.R. and Fravrat D., February 1998. Flow Boiling in Horizontal Tubes: Part I - Development of a Diabatic Two-Phase Flow Pattern map, Journal of Heat Transfer, vol. 120, pg. 140-147.
- [6] Cavallini A., Censi G., Del Col D., Doretti L., Longo G.A. and Rossetto L., 2001. Experimental Investigation on Condensation Heat Transfer and Pressure Drop of New HFC Refrigerants (R134a, R125, R32, R410A R236ea) in a Horizontal Smooth Tube, Int. Journal of Refrigeration, vol. 24, pg. 73-87.
- [7] Jung D.S. and Didion A., 1989. Electrical Power Research Institute (EPRI) ER- 6364, Research Project 8006-2.
- [8] Rigola J., Pérez Segarra C.D., and Oliva A., 2003. Modelling and numerical simulation of the thermal and fluid dynamic behaviour of hermetic reciprocating compressors - part 2: Experimental investigation. Int. Journal of Heating Ventilating Air Conditioning and Refrigeration Research, 9(2), pg. 237– 250.
- [9] Wong Y.L., Groeneveld D.C. and Cheng S.C., 1990. CHF prediction for horizontal tubes. Int. Journal of Multiphase Flow, 16, pg. 123-138.
- [10] Michael F. Modest. Radiative Heat Transfer. McGraw Hill, 1993.
- [11] Toshiyuki Miyayama and Yukio Nakano. Radiation heat transfer in three dimensional closed space including diffuse and specular surfaces. Heat Transfer - Asian Research, vol 32(2) 2003, p. 108-129.
- [12] Nicoud F. and F. Ducros, 1999. *Subgrid-scale stress modelling based on the square of the velocity gradient tensor*. Flow, Turbulence and Combustion, 62:183–200.
- [13] Verstappen R.W.C.P. and Van Der Velde R.M., Symmetry-Preserving Discretization of Heat Transfer in a Complex Turbulent Flow, Journal of Engineering Mathematics 54 (4) (2006) 299-318.
- [14] Chiva J., Ventosa J., Lehmkuhl O. and Pérez-Segarra C.D., Modelization of the Low-Mach Navier Stokes Equations in Unstructured Meshes, Proceedings of the 7th International conference on computational heat and mass transfer (2011).
- [15] Borrell R., Lehmkuhl O., Trias F. and Oliva A., Parallel direct Poisson solver for discretisations with one Fourier diagonalisable direction, Computational Physics, Vol. 230, No. 12, 2011, pp. 4723-4741.
- [16] Trias F.X., Soria M., Pérez-Segarra C.D. and Oliva A., Direct numerical simulation of a three-dimensional natural convection flow in a differentially heated cavity of aspect ratio 4, Numerical Heat Transfer part A-Applications 45 (2004) 649-673.